

NOMA versus OMA in Finite Blocklength Regime: Link-Layer Rate Performance

Muhammad Amjad, Leila Musavian, and Sonia Aïssa

Abstract—In this paper, we investigate the latency performance comparison of non-orthogonal multiple access (NOMA) and orthogonal multiple access (OMA) in finite blocklength regime. In this regard, we derive the achievable effective capacity of a two-users NOMA network, and its OMA counterpart, under delay quality-of-service constraints. We, then, obtain closed-form expressions for the achievable effective capacity of the weak and strong users in Rayleigh fading channels. Through simulations, we show that at low signal-to-noise ratios (SNRs), the OMA user with better channel condition outperforms both NOMA users. The comparative analysis of total link-layer rate shows that at high SNRs, when the delay exponent is loose, the total link-layer rate of NOMA with finite blocklength outperforms the one of OMA.

Index Terms—NOMA, OMA, effective capacity, finite blocklength, low-latency communications.

I. INTRODUCTION

Transition from the ultra-low latency to the massive ultra-reliable and low latency communications (mURLLC) for beyond 5th generation (B5G) applications demands the researchers from both industry and academia to revisit the enabling technologies. Future smart cities, autonomous robotics, holographic communications, blockchain, and massive sensing, are few examples to name that require the mURLLC service class of B5G [1]. Achieving mURLLC for the above-mentioned future applications is indeed a challenging task. While the non-orthogonal multiple access (NOMA) in conjunction with finite blocklength (short packet) communications is considered as an enabler of low-latency communications [2], further research is required to quantify the end-to-end latency in these systems. Also, the scalability of this technology is yet to be investigated.

NOMA with finite blocklength can promise ultra-low latency, massive connectivity, and higher throughput under favorable conditions [3]. The principle NOMA in finite blocklength regime follows the traditional concept of NOMA, with superposition coding (SC) at the transmitter and successive interference cancellation (SIC) at the receiver [4]. However, when operating with finite blocklength packets, the Shannon formula is not a good approximate for the achievable rate of the NOMA. For this purpose, the authors in [5] provided a framework to approximate the achievable rate of a point-to-point communication link in finite blocklength regime.

Can the latency requirements of mURLLC for B5G services be satisfied with NOMA in finite blocklength regime?

This question needs a detailed delay performance analysis of NOMA in finite blocklength regime. In this regard, the authors in [3] investigated the performance of NOMA with short packet communications for a given reliability constraint. More specifically, this work showed the reduction in physical-layer transmission latency while using NOMA in conjunction with short packet communications. The latency performance of NOMA with finite blocklength regime was further investigated in [4], which confirmed the improved performance of NOMA in terms of reducing latency and improving throughput, in comparison to its orthogonal multiple access (OMA) counterpart. Motivated by above works, in this paper, we investigate the latency performance of NOMA and OMA in a short packet communication regime. We derive the achievable EC of a two-users¹ NOMA and an OMA in finite blocklength regime. Specifically in this work, (i) the achievable EC (link-layer rate) of NOMA users is investigated in finite blocklength regime under heterogeneous delay quality-of-service (QoS) requirements, in comparison with the OMA counterpart, (ii) we further derive closed-form expressions for the individual users' EC in the two-users NOMA and OMA networks, and (iii) we show that the OMA user with better channel conditions outperforms both NOMA users at low SNRs, while the total link-layer rate of NOMA outperforms the one of OMA under loose delay constraints.

II. TRANSMISSION FRAMEWORK AND FUNDAMENTALS

We consider a downlink two-users NOMA network with finite blocklength. The users, denoted by v_i , $i = \{1, 2\}$, are equipped with single antennas and communicate with a single base station (BS). The channel coefficient between the BS and v_i at time τ is referred to by $h_i(\tau)$. The two users are classified based on their channel conditions as strong and weak users and, while without loss of generality, we assume $|h_1(\tau)|^2 \geq |h_2(\tau)|^2$. Following the NOMA operation, the BS broadcasts a combined message $\sum_{i=1}^2 \sqrt{\alpha_i P} u_i(\tau)$ to its users, where u_i is the message corresponding to user v_i , P is the BS total transmit power, and α_i is the power coefficient for user v_i . The power coefficients for the two users are such that $\alpha_1 \leq \alpha_2$. The received signal at user v_i can now be formulated as² $y_i = h_i \sum_{i=1}^2 \sqrt{\alpha_i P} s_i + m_i$, where m_i is the additive white Gaussian noise (AWGN) at v_i , $i = \{1, 2\}$. The strong user (v_1) first performs the SIC to remove interference

M. Amjad and L. Musavian are with the School of Computer Science and Electronic Engineering, University of Essex, CO4 3SQ, UK (Email: {m.amjad, leila.musavian}@essex.ac.uk). S. Aïssa is with the Institut National de la Recherche Scientifique (INRS-EMT), University of Quebec, Montreal, QC, H5A 1K6, Canada (Email: aissa@emt.inrs.ca).

¹A two-users NOMA network has been included in third generation partnership project long-term evolution advanced (3GPP-LTE-A) networks and is considered as an elementary block of NOMA [3].

²As the channel coefficients are assumed stationary and ergodic random processes, the time index τ is omitted hereafter for simplicity of presentation.

(u_2) from its received signal (y_1), and then, decodes its own message. Therefore, the received signal-to-noise ratio (SNR) at v_1 , denoted SNR_1^N ,³ can be found as

$$\text{SNR}_1^N = \alpha_1 \rho |h_1|^2, \quad (1)$$

where ρ is the transmit SNR, namely $\rho = \frac{P}{N_o B}$, in which $N_o B$ denotes the noise power. On the other hand, the weak user (v_2) treats u_1 as interference and decodes its own message directly. Hence, the resulting signal-to-interference-plus-noise ratio (SINR) at v_2 can be derived as,

$$\text{SINR}_2^N = \frac{\alpha_2 \rho |h_2|^2}{\alpha_1 \rho |h_2|^2 + 1}. \quad (2)$$

Channel gains of both users are modeled as Rayleigh distribution with unit variance. Following the NOMA operation, the users v_1 and v_2 are sorted based on their ordered channel gains. Therefore, the probability density function (PDF) of the ordered channel power gains can be obtained using the order statistics [6]. In this regard, using $\rho |h_i|^2 = \gamma_i$ and denoting its PDF as $f(\gamma_i)$, we apply the order statistics to get

$$f_{\gamma_{1:2}}(\gamma_1) = \xi_1 f(\gamma_1) F(\gamma_1), \quad f_{\gamma_{2:2}}(\gamma_2) = \xi_2 f(\gamma_2) (1 - F(\gamma_2)), \quad (3)$$

where $f_{\gamma_{i:2}}$ is the PDF of the ordered γ_i out of two users, and $\xi_i = \frac{1}{B(i, 2-i+1)}$, in which $B(a, b)$ is the beta function [7]. Further, we assume the two-users can operate in OMA. In this regard, both users are given the same spectrum bandwidth as in the NOMA technique but each user can only occupy half of the time slot. As aforementioned, in this work we consider the finite blocklength communication regime with NOMA or OMA. Therefore, the users' achievable rates, in the NOMA and OMA cases, can be formulated using the results of [5], and expressed in b/s/Hz, as

$$r_1^N = \log_2(1 + \alpha_1 \gamma_1) - \sqrt{\frac{V_1^N}{n}} Q^{-1}(\epsilon), \quad (4)$$

$$r_2^N = \log_2\left(1 + \frac{\alpha_2 \gamma_2}{\alpha_1 \gamma_2 + 1}\right) - \sqrt{\frac{V_2^N}{n}} Q^{-1}(\epsilon), \quad (5)$$

$$r_i^O = \frac{1}{2} \left(\log_2(1 + \gamma_i) - \sqrt{\frac{V_i^O}{n}} Q^{-1}(\epsilon) \right), \quad i = \{1, 2\}, \quad (6)$$

where r_1^N , r_2^N and r_i^O are the achievable rates for the NOMA strong user, NOMA weak user, and OMA users, respectively, n is the blocklength, ϵ is the transmission error probability, and $Q^{-1}(\cdot)$ is the inverse of Gaussian Q-function with $Q(x) = \int_x^\infty \frac{1}{\sqrt{2\pi}} e^{-\frac{w^2}{2}} dw$. Also, $V_1^N = \sqrt{1 - (1 + \alpha_1 \gamma_1)^{-2}}$, $V_2^N = \sqrt{1 - \left(1 + \frac{\alpha_2 \gamma_2}{\alpha_1 \gamma_2 + 1}\right)^{-2}}$, and $V_i^O = \sqrt{1 - (1 + \gamma_i)^{-2}}$ are the channel dispersions of the NOMA strong user, NOMA weak user, and OMA users, respectively.

A. Theory of Effective Capacity

In this subsection, we explain the basic concepts related to the theory of EC. This metric used to find the maximum

arrival rate for a given service rate while satisfying a certain delay-outage probability constraint [8]. We assume that the transmission scheme in our network is required to satisfy a statistical delay QoS constraints. It is shown that if a queue length exceeds a certain threshold (x), then by using the large deviation theorem [9] the probability of the buffer overflow will hold the following equality

$$-\lim_{x \rightarrow \infty} \frac{\ln(\Pr\{q_i(\infty) > x\})}{x} = \theta_i, \quad (7)$$

where $q_i(\infty)$ is the steady-state transmit buffer of user v_i , θ_i is this user's delay exponent, and $\Pr\{a > b\}$ is the probability that $a > b$ holds. Following (7), the queueing delay violation probability can be estimated as [8]

$$\Pr\{D_i > D_{\max}^i\} \approx \Pr\{q_i(\infty) > 0\} e^{-\theta_i \mu_i D_{\max}^i}, \quad i = \{1, 2\}, \quad (8)$$

where, for user v_i , D_{\max}^i is the maximum delay, $\Pr\{q_i(\infty) > 0\}$ is the probability of non-empty buffer, and μ_i is the maximum arrival rate, according to EC [8].

III. EFFECTIVE CAPACITY OF NOMA AND OMA IN FINITE BLOCKLENGTH REGIME

In this section, we derive the achievable EC of a two-users NOMA and OMA network in finite blocklength communication regime. We then provide closed-form expressions for the EC. By following the stochastic model for the achievable EC in [10], [11], the achievable EC for the two-users NOMA and the OMA counterpart, in finite blocklength regime can therefore be formulated as

$$C_i^N = -\frac{1}{\theta_i n} \ln\left(\mathbb{E}[\epsilon + (1 - \epsilon) e^{-\theta_i n r_i^N}]\right), \quad (9)$$

$$C_i^O = -\frac{1}{\theta_i n} \ln\left(\mathbb{E}[\epsilon + (1 - \epsilon) e^{-\theta_i n r_i^O}]\right), \quad (10)$$

where C_i^N and C_i^O represent the EC of user v_i in a finite blocklength regime, for NOMA and OMA, respectively, $\mathbb{E}[\cdot]$ is the expectation operator. By considering the service rate r_i^N for the users v_i in finite blocklength regime from (4) and (5), the achievable EC for the NOMA strong user and the NOMA weak user can be approximated as

$$C_1^N = -\frac{1}{\theta_1 n} \ln\left(\mathbb{E}[\epsilon + (1 - \epsilon) (1 + \alpha_1 \gamma_1)^{2\Upsilon_1} e^{\psi_1 V_1^N}]\right), \quad (11)$$

$$C_2^N = -\frac{1}{\theta_2 n} \ln\left(\mathbb{E}[\epsilon + (1 - \epsilon) \left(1 + \frac{\alpha_2 \gamma_2}{\alpha_1 \gamma_2 + 1}\right)^{2\Upsilon_2} e^{\psi_2 V_2^N}]\right), \quad (12)$$

where $\Upsilon_i = -\frac{\theta_i n}{2 \ln 2}$, and $\psi_i = \theta_i \sqrt{n} Q^{-1}(\epsilon)$. On the other hand, we assume that both users, v_1 and v_2 , can also operate according to OMA, by transmitting their messages using time division multiple access (TDMA). Then, using (6), the achievable EC of the two OMA users can be approximated as

$$C_i^O = -\frac{1}{\theta_i n} \ln\left(\mathbb{E}[\epsilon + (1 - \epsilon) (1 + \gamma_i)^{\Upsilon_i} e^{\frac{\psi_i V_i^O}{2}}]\right). \quad (13)$$

The above derived individual EC expressions of a two-users NOMA and OMA in finite blocklength regime can be used to investigate the comparative analysis of delay performance for NOMA and OMA. However, to further simplify the above expressions, we derive closed-form expressions for the individual

³Superscript N indicates NOMA. Later, notation O will be used to indicate the OMA operation.

$$C_1^N = -\frac{1}{\theta_1 n} \ln \left(\epsilon + (1 - \epsilon) \frac{2}{\alpha_1 \rho} e^{\psi_1} \left(H \left(1, 2 + 2\Upsilon_1, \frac{1}{\alpha_1 \rho} \right) - H \left(1, 2 + 2\Upsilon_1, \frac{2}{\alpha_1 \rho} \right) \right) \right). \quad (14)$$

$$C_2^N = -\frac{1}{\theta_2 n} \ln \left(\epsilon + (1 - \epsilon) \frac{2\alpha_1^{-2\Upsilon_2}}{\rho} e^{\psi_2} \left(H \left(1, 2, \frac{2}{\rho} \right) + \frac{n\theta_2(\alpha_1 - 1)}{\alpha_1 \ln 2} e^{\frac{2}{\alpha_1 \rho}} E_i \left(-\frac{2}{\alpha_1 \rho} \right) + \sum_{k=2}^{\infty} \binom{2\Upsilon_2}{k} \left(\frac{\alpha_1 - 1}{\alpha_1} \right)^k \right. \right. \\ \left. \left. \times \left(\frac{\sum_{j=1}^{k-1} \frac{(j-1)!}{\alpha_1^{-j}} \left(-\frac{2}{\rho} \right)^{k-j-1} - \left(-\frac{2}{\rho} \right)^{k-1}}{(k-1)!} e^{\frac{2}{\alpha_1 \rho}} E_i \left(-\frac{2}{\alpha_1 \rho} \right) \right) \right) \right). \quad (15)$$

$$C_1^O = -\frac{1}{\theta_1 n} \ln \left(\epsilon + (1 - \epsilon) \frac{2}{\rho} e^{\frac{\psi_1}{2}} \left(H \left(1, 2 + \Upsilon_1, \frac{1}{\rho} \right) - H \left(1, 2 + \Upsilon_1, \frac{2}{\rho} \right) \right) \right). \quad (16)$$

$$C_2^O = -\frac{1}{\theta_2 n} \ln \left(\epsilon + (1 - \epsilon) \frac{2}{\rho} e^{\frac{\psi_2}{2}} H \left(1, 2 + \Upsilon_2, \frac{1}{\rho} \right) \right). \quad (17)$$

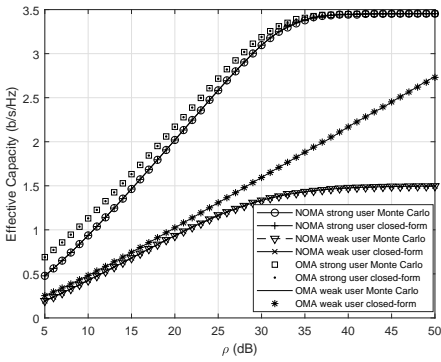


Fig. 1. Achievable EC of a two-users NOMA and OMA versus the transmit SNR.

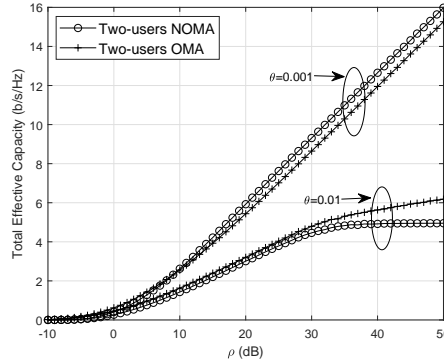


Fig. 2. Total achievable EC of a two-users NOMA and OMA versus the transmit SNR.

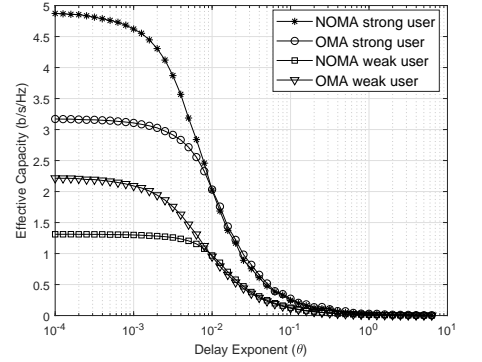


Fig. 3. Achievable EC of a two-users NOMA and OMA, versus delay exponent (θ).

EC of the strong and weak NOMA and OMA users in finite blocklength regime. Specifically, using the order statistics from (3), the final closed-form expressions for the two-users NOMA and OMA can be obtained as shown in (14) to (17). The proofs for the derived closed-form expressions for C_1^N , C_1^O and C_2^O are provided in Appendix A, while the proof for deriving the closed-form expression for C_2^N is presented in Appendix B.

IV. NUMERICAL RESULTS

In this section, we perform extensive simulations to investigate the performance comparison of the two-users NOMA and OMA in finite blocklength regime. The users' power coefficients are $\alpha_2 = 0.7$ and $\alpha_1 = 0.3$, the blocklength is $n = 400$, and the transmission error probability $\epsilon = 10^{-6}$, unless otherwise specified.

Fig. 1 shows the plots of the achievable EC of a two-users NOMA and OMA in a finite blocklength regime versus the transmit SNR (ρ) in dB. For this evaluation, we set $\theta = 0.01$. The accuracy of the derived closed-form expressions is confirmed. The figure also shows that, at very low transmit SNRs, OMA strong user outperforms both NOMA users. However, as ρ tends to increase, the achievable EC of NOMA and OMA does not increase further and saturates at very high values of the SNR. At low SNRs, the achievable EC of the weak user are approximately the same in both NOMA and OMA, whereas at high SNRs the weak user OMA dominates with a big gap. Fig.

2 shows the plots of the total achievable EC of a two-users NOMA and OMA versus the transmit SNR (ρ). The results reveal that the total achievable rate of NOMA outperforms the one for OMA at high SNRs when $\theta = 0.001$. On the other hand, when the delay exponent becomes stringent, i.e., changes from $\theta \rightarrow 0.001$ to $\theta \rightarrow 0.01$, the total link-layer rate of OMA outperforms the one of NOMA at high SNRs. However, at the low SNRs, the total link-layer rate of NOMA and OMA are approximately the same irrespective of the delay constraints. Fig. 3 shows the simulation results of individual user's achievable EC of a two-user NOMA and OMA versus the delay exponent θ when the transmit SNR $\rho = 20$ dB. This figure shows that the NOMA users outperform the OMA users when the delay exponent is very loose. However, when the delay exponent becomes stringent, the NOMA users show a considerable loss in EC as compared to the OMA users. These results reveal that, as compared to the NOMA users, OMA users in a finite blocklength can perform better under stringent delay QoS requirements.

V. CONCLUSION

In this paper, we formulated the individual user's achievable EC of a two-users NOMA and OMA in finite blocklength regime. We derived closed-form expressions for the individual EC of both users, in NOMA and OMA, and confirmed their accuracy using Monte-Carlo simulations. We investigated the

performance comparison of NOMA and OMA users through simulations under heterogeneous delay QoS constraints. The performance comparison showed that at low SNRs the strong user OMA outperforms both NOMA users, while the total link-layer rate of NOMA outperforms the one of OMA at high SNRs.

APPENDIX A

To obtain the closed-form expressions for C_1^N , C_1^O , and C_2^O , we first consider the simple case of C_1^O and derive its closed-form expression. In this regard, following the order statistics from (3), C_1^O (from (13)) can be expanded as

$$C_1^O = -\frac{1}{\theta_1 n} \ln \left(\int_0^\infty \left(\epsilon + (1-\epsilon)(1+\gamma_1)^{\Upsilon_1} e^{-\frac{\psi_1 V_1^O}{2}} \right) \times f_{\gamma_{1:2}}(\gamma_1) d\gamma_1 \right), \quad (18)$$

where $f(\gamma_1) = \frac{1}{\rho} e^{-\frac{\gamma_1}{\rho}}$, $F(\gamma_1) = 1 - e^{-\frac{\gamma_1}{\rho}}$, and we assume at high SNR $V_i^N \approx 1$, $V_i^O \approx 1$ [5], we get

$$C_1^O = -\frac{1}{\theta_1 n} \ln \left(\epsilon + (1-\epsilon) \frac{2}{\rho} e^{\frac{\psi_1}{2}} \underbrace{\left(\int_0^\infty (1+\gamma_1)^{\Upsilon_1} e^{-\frac{\gamma_1}{\rho}} d\gamma_1 \right)}_{I_1} - \underbrace{\int_0^\infty (1+\gamma_1)^{\Upsilon_1} e^{-\frac{2\gamma_1}{\rho}} d\gamma_1}_{I_2} \right), \quad (19)$$

We now introduce the equality from [eq (13.2.5) [7]]

$$H(a, b, z) = \frac{1}{\Gamma(a)} \int_0^\infty e^{-zt} t^{a-1} (1+t)^{b-a-1} dt \quad (20)$$

where $H(\cdot, \cdot, \cdot)$ is the confluent hypergeometric function of the second kind [7]. By using (20), the integrals I_1 and I_2 can be solved as

$$I_1 = H\left(1, 2 + \Upsilon_1, \frac{1}{\rho}\right), \quad I_2 = H\left(1, 2 + \Upsilon_1, \frac{2}{\rho}\right). \quad (21)$$

Inserting (21) into (19), the closed-form expression for C_1^O can finally be derived as is given in (16). Similarly, following the above steps, the closed-form expressions for C_1^N and C_2^O (given in (14) and (17)) can also be obtained.

APPENDIX B

Following the order statistics from (3), achievable EC of the weak NOMA user from (12) can be expanded as

$$C_2^N = -\frac{1}{\theta_2 n} \ln \left(\int_0^\infty \left(\epsilon + (1-\epsilon) \left(\frac{\gamma_2 + 1}{\alpha_1 \gamma_2 + 1} \right)^{2\Upsilon_2} \times e^{\psi_2 V_2^N} \right) f_{\gamma_{2:2}}(\gamma_2) d\gamma_2 \right), \quad (22)$$

where $f(\gamma_2) = \frac{1}{\rho} e^{-\frac{\gamma_2}{\rho}}$, $F(\gamma_2) = 1 - e^{-\frac{\gamma_2}{\rho}}$, and we assume at high SNR $V_2^N \approx 1$ [5], we get

$$C_2^N = -\frac{1}{\theta_2 n} \ln \left(\epsilon + (1-\epsilon) \frac{2}{\rho} e^{\psi_2} \int_0^\infty \left(\frac{\gamma_2 + 1}{\alpha_1 \gamma_2 + 1} \right)^{2\Upsilon_2} e^{-\frac{2\gamma_2}{\rho}} d\gamma_2 \right). \quad (23)$$

Following the generalized binomial expansion, we can write $\left(\frac{\gamma_2 + 1}{\alpha_1 \gamma_2 + 1} \right)^{2\Upsilon_2} = \left(\frac{1}{\alpha_1} \right)^{2\Upsilon_2} \left(1 + \frac{\alpha_1 - 1}{\alpha_1 \gamma_2 + 1} \right)^{2\Upsilon_2}$, where the expression $\left(1 + \frac{\alpha_1 - 1}{\alpha_1 \gamma_2 + 1} \right)^{2\Upsilon_2}$ can further be expanded as $\left(1 + \frac{\alpha_1 - 1}{\alpha_1 \gamma_2 + 1} \right)^{2\Upsilon_2} = \sum_{k=0}^\infty \binom{2\Upsilon_2}{k} \left(\frac{\alpha_1 - 1}{\alpha_1 \gamma_2 + 1} \right)^k$. Using the above expansions, (23) can be transformed into

$$C_2^N = -\frac{1}{\theta_2 n} \ln \left(\epsilon + (1-\epsilon) \frac{2\alpha_1^{-2\Upsilon_2}}{\rho} e^{\psi_2} \underbrace{\left(\int_0^\infty e^{-\frac{2\gamma_2}{\rho}} d\gamma_2 \right)}_{I_a (k=0)} + \underbrace{\int_0^\infty 2\Upsilon_2 \frac{\alpha_1 - 1}{\alpha_1 \gamma_2 + 1} e^{-\frac{2\gamma_2}{\rho}} d\gamma_2}_{I_b (k=1)} + \underbrace{\int_0^\infty \sum_{k=2}^\infty \binom{2\Upsilon_2}{k} \left(\frac{\alpha_1 - 1}{\alpha_1 \gamma_2 + 1} \right)^k e^{-\frac{2\gamma_2}{\rho}} d\gamma_2}_{I_c (k \geq 2)} \right). \quad (24)$$

Using (20), we get, $I_a = H\left(1, 2, \frac{2}{\rho}\right)$. For the integrals I_b and I_c , we use (3.353.2) and (3.352.4) from [12] such that,

$$\int_0^\infty \frac{e^{-zt}}{t+b} dt = -e^{bz} \text{Ei}(-bz), \quad [\arg b] < \pi, \quad \text{Re}(z) > 0, \quad (25)$$

$$\int_0^\infty \frac{e^{-zt}}{(t+b)^n} dt = \frac{1}{(n-1)!} \sum_{j=1}^{n-1} (j-1)! (-z)^{n-j-1} (b^{-j}) - \frac{(-z)^{n-1}}{(n-1)!} e^{bz} \text{Ei}(-bz), \quad [n \geq 2, \arg b] < \pi, \text{Re } z > 0, \quad (26)$$

where $\text{Ei}(\cdot)$ is the exponential integral [12]. Using (25) and (26), the closed-form expression for C_2^N can be derived as given in (15).

REFERENCES

- [1] W. Saad, M. Bennis, and M. Chen, "A vision of 6G wireless systems: Applications, trends, technologies, and open research problems," *arXiv preprint arXiv:1902.10265*, Jul. 2019.
- [2] M. Amjad and L. Musavian, "Performance analysis of NOMA for ultra-reliable and low-latency communications," in *IEEE Globecom Workshops (GC Wkshps)*, Abu Dhabi, Dec. 2018, pp. 1–5.
- [3] Y. Yu, H. Chen, Y. Li, Z. Ding, and B. Vucetic, "On the performance of non-orthogonal multiple access in short-packet communications," *IEEE Commun. Lett.*, vol. 22, no. 3, pp. 590–593, Mar. 2018.
- [4] E. Dosti, M. Shehab, H. Alves, and M. Latva-aho, "On the performance of non-orthogonal multiple access in the finite blocklength regime," *Ad Hoc Netw.*, vol. 84, pp. 148–157, Mar. 2019.
- [5] Y. Polyanskiy, H. V. Poor, and S. Verdú, "Channel coding rate in the finite blocklength regime," *IEEE Trans. Inf. Theory*, vol. 56, no. 5, pp. 2307–2359, May 2010.
- [6] H. A. David and H. N. Nagaraja, "Order statistics," *Encyclopedia of Statistical Sciences*, 2004.
- [7] M. Abramowitz and I. A. Stegun, "Handbook of mathematical functions dover publications," New York, p. 361, 1965.
- [8] M. Amjad, L. Musavian, and M. H. Rehmani, "Effective capacity in wireless networks: A comprehensive survey," *IEEE Commun. Surveys Tuts.*, 2019.
- [9] C.-S. Chang, *Performance guarantees in communication networks*. Springer Science & Business Media, 2012.
- [10] M. C. Gursoy, "Throughput analysis of buffer-constrained wireless systems in the finite blocklength regime," *EURASIP J. Wireless Commun. Net.*, vol. 2013, no. 1, p. 290, Dec. 2013.
- [11] M. Shehab, H. Alves, and M. Latva-aho, "Effective capacity and power allocation for machine-type communication," *IEEE Trans. Veh. Technol.*, vol. 68, no. 4, pp. 4098–4102, Apr. 2019.
- [12] I. S. Gradshteyn and I. M. Ryzhik, *Table of integrals, series, and products*. Academic press, 2014.